Publishing Excellence Inspiring Progress
ARISTON PUBLICATIONS
Energy & Environment Advances
ISSN: 3066-5728 https://aristonpubs.com/energy-environment-advances https://doi.org/10.69626/eea.2025.0122

RESEARCH ARTICLE

Room–Temperature Acetone Detection Using SILAR–Synthesized Polyaniline Thin Film Sensors

Pratik Kamtekar [1], Ankita P. Angre [2], Pratap Patil [2], Priya A. Patil [3], Rohit Mahadule [4], Gayatri S. Bhagwat [5], Paresh S. Gaikar [1,*]

ABSTRACT: The demand for precise, real-time monitoring of volatile organic compounds such as acetone has driven significant research into advanced gas sensing technologies. Conventional metal oxide sensors typically require elevated operating temperatures, which impose constraints on energy efficiency and device portability. In this work, we present a viable alternative through the development of polyaniline (PANI) thin films fabricated via the Successive Ionic Layer Adsorption and Reaction (SILAR) technique, designed specifically for room-temperature acetone sensing. Comprehensive material characterization was conducted using X-ray diffraction (XRD), scanning electron microscopy (SEM), and ultraviolet-visible (UV-Vis) spectroscopy. These analyses verified the semicrystalline nature and porous nanoscale morphology of the PANI films, which are instrumental in facilitating effective gas adsorption. The sensor demonstrated pronounced selectivity toward acetone, exhibiting an 85% response, substantially higher than that for methanol, ammonia, and formaldehyde. Concentration-dependent studies revealed a progressive increase in sensitivity, reaching 85% at 100 ppm acetone. The dynamic sensing performance showed a response time of approximately 219.6 seconds and a recovery time of about 444.4 seconds, indicative of favorable adsorption-desorption kinetics. These results underscore the potential of SILAR-deposited PANI thin films as selective, energy-efficient, and room-temperature operable sensors for acetone detection. Such sensors hold considerable promise for applications in non-invasive medical diagnostics, such as diabetes breath analysis, and in continuous environmental air quality monitoring.

Keywords: Polyaniline, SILAR Method, Acetone Sensor, Thin Film, Gas Selectivity, Room-Temperature Sensing.

Received: 28 January 2025; Revised: 21 April 2025; Accepted: 19 May 2025; Published Online: 26 July 2025

1. INTRODUCTION

The pervasive existence of gases, ranging from life-sustaining oxygen to hazardous industrial pollutants, underscores a critical global need for advanced gas sensing technologies. Reliable detection and continuous monitoring are indispensable across a multitude of sectors, including industrial process control, environmental protection, and healthcare diagnostics [1-3]. The ability to provide precise, real-time data on atmospheric composition is fundamental for ensuring workplace safety, optimizing manufacturing efficiency, and enforcing regulatory standards for air quality. This imperative becomes particularly pronounced when addressing volatile organic compounds (VOCs), a vast class of carbon-based chemicals that readily evaporate at ambient conditions. Emitted from numerous sources such as vehicle exhaust, industrial solvents, building materials, and even natural biological processes, VOCs pose significant challenges due to their diversity, ubiquitous presence, and potential adverse effects on human health and the environment [4-6]. Consequently, the development of robust, sensitive, and selective sensors capable of identifying

[1] Rayat Shikshan Sanstha's, Karmaveer Bhaurao Patil College, Vashi, Navi Mumbai, 400703, Maharashtra, India.
[2] Ramnarain Ruia Autonomous College, Matunga, Mumbai, 400019, Maharashtra, India.
[3] Changu Kana Thakur A. C. S. College, New Panvel-410206, Maharashtra, India.
[4] S. Chandra Mahila Mahavidyalaya, Sadak Arjuni, Gondia, 441807, Maharashtra, India,
[5] Mahatma Phule A.S.C. College, Panvel, Raigad, 410206, Maharashtra, India

* Author to whom correspondence should be addressed: psgaikar@kbpcollege.edu.in (Paresh S. Gaikar)

© Ariston Publications 2025. All rights reserved.

specific VOCs within complex mixtures is a central focus of materials science and sensor engineering.

Among the plethora of VOCs, acetone (C_3H_6O) emerges as a molecule of exceptional interest for targeted detection. Its extensive use as a solvent in laboratories and industries like pharmaceuticals and plastics manufacturing necessitates vigilant monitoring to prevent occupational exposure and environmental contamination [7]. Beyond its industrial footprint, acetone holds profound significance in medical diagnostics. It is a key metabolite in the human body, and its concentration in exhaled breath serves as a vital, non-invasive biomarker for metabolic disorders, most notably diabetes mellitus. Elevated breath acetone levels correlate strongly with diabetic ketoacidosis, a serious complication, making its detection a promising tool for disease management and screening [8]. Furthermore, acetone's high vapor pressure and flammability demand careful handling and leak detection in storage and transport settings [9-11]. These multifaceted roles, from industrial workhorse to diagnostic marker, create an urgent and growing demand for acetone sensors that are not only highly sensitive but also capable of distinguishing acetone from interfering gases commonly found in ambient air, such as ethanol, methanol, and formaldehyde.

The quest for such performance, however, encounters a significant technological hurdle, particularly concerning operational energy requirements. For decades, chemiresistive gas sensors based on metal oxide semiconductors (MOS), such as tin oxide (SnO_2) or tungsten oxide (WO_3), have dominated the field. Their sensing mechanism relies on changes in electrical resistance induced by the adsorption and desorption of gas molecules on their surface. A fundamental limitation of most MOS materials is that this redox process requires elevated thermal energy to proceed at a useful rate and sensitivity. Consequently, these sensors typically incorporate integrated micro-heaters to operate at temperatures between 200°C and 450°C [12]. This requisite for high-temperature activation leads to substantial power consumption, complicates device design, limits battery life in portable systems, and raises safety concerns in potentially explosive atmospheres. The need for heating elements also hinders the integration of sensors into flexible, wearable, or large-area distributed network applications, where low power budgets and mechanical conformity are paramount [2].

In this context, conductive polymers have surfaced as a compelling alternative platform for next-generation gas sensors. Polyaniline (PANI) stands out due to its unique combination of advantageous properties. It exhibits tunable electrical conductivity, which can be modulated through doping and dedoping processes. Its rich redox chemistry and π-conjugated electron system allow for direct, room-temperature interaction with analyte molecules. Upon exposure to gases like acetone, the physical adsorption and subsequent charge transfer between the gas and the polymer backbone induce a measurable change in the film's electrical resistance, without the need for external thermal activation [13, 14]. This intrinsic room-temperature activity is a transformative advantage, enabling the development of truly low-power sensing devices. Additionally, PANI is amenable to solution processing, can be deposited on flexible substrates, and is compatible with printing techniques, thereby opening avenues for inexpensive, lightweight, and conformable sensor fabrication [2].

The performance of a PANI-based sensor is intrinsically linked to its nanoscale morphology and film architecture. A high surface-to-volume ratio and a porous structure are crucial as they maximize the active sites available for gas interaction and facilitate the rapid diffusion of analyte molecules throughout the sensing layer. Therefore, the chosen deposition method must offer precise control over these critical parameters. This investigation employs the Successive Ionic Layer Adsorption and Reaction (SILAR) technique for the synthesis of PANI thin films [15]. SILAR is a solution-based, cyclic deposition method renowned for its simplicity, cost-effectiveness, and suitability for coating large or complex substrates. Its layer-by-layer growth mechanism allows for exceptional control over film thickness, density, and morphology by simply varying the number of deposition cycles and the composition of the precursor solutions [16-18]. This capability to engineer a nanostructured, porous film at near-ambient temperatures is a key advantage of the SILAR process. The novelty of this work lies in the synergistic application of the SILAR technique to engineer nanostructured PANI thin films specifically tailored for selective acetone detection at room temperature, a approach that directly addresses the energy and selectivity limitations of conventional sensing platforms while leveraging a scalable and controllable fabrication method.

While the potential of conductive polymers is clear, the performance landscape of reported sensors is varied. For comparison, a typical MOS sensor for ethanol demonstrated rapid kinetics with a 32-second response and 14-second recovery time, albeit at high operating temperatures [19]. PANI-based composites have shown extraordinary sensitivity, such as a 2150% response to 10 ppm ammonia, and impressive detection limits reaching parts-per-billion levels [20]. Some PANI configurations have also achieved fast response and recovery times on the order of one to two minutes for ammonia sensing [21]. However, challenges persist, particularly regarding the selectivity toward specific VOCs and the sometimes protracted recovery times due to strong chemical interactions, which can hinder sensor reversibility and long-term stability [22]. Therefore, a dedicated effort to optimize the material synthesis and film structure to favor selective and reversible acetone interaction is warranted. Prior studies have utilized various techniques to characterize PANI; for instance, X-ray diffraction (XRD) consistently reveals the semicrystalline nature of polyaniline in its emeraldine salt form, a state essential for its conductivity [23]. Scanning electron microscopy (SEM) further elucidates the morphology, often showing fibrous or granular structures that contribute to a high surface area [23, 24]. The successful application of SILAR to create functional PANI films for other applications, such as supercapacitor electrodes, supports its viability for sensor fabrication [25]. Building upon this foundation, the present study

© Ariston Publications 2025. All rights reserved.

systematically employs SILAR to deposit PANI thin films, followed by rigorous characterization using XRD, SEM, and UV-Vis spectroscopy to correlate the material's physical and optical properties with its gas sensing performance. The ultimate goal is to demonstrate a sensor that combines the room-temperature operation of conductive polymers with the tailored morphology enabled by SILAR processing, thereby achieving a sensitive, selective, and energy-efficient platform for acetone detection with practical utility in breath analysis and environmental monitoring.

2. EXPERIMENTAL DETAILS

2.1. Materials and Chemicals

All chemicals utilized in this synthesis were of analytical reagent (A.R.) grade and employed without additional purification. The aniline monomer ($C_6H_5NH_2$) served as the primary precursor for polymerization. Sulfuric acid (H_2SO_4, 0.2 M) functioned as both the reaction medium and the primary dopant to yield the conductive emeraldine salt form of polyaniline. Ammonium persulfate ($(NH_4)_2S_2O_8$, 0.5 M) was used as the oxidizing agent to initiate and propagate the polymerization reaction. Nitric acid (HNO_3) and hydrochloric acid (HCl) were available for pH adjustment and cleaning procedures. All aqueous solutions were prepared using doubly distilled water to minimize the influence of ionic contaminants on the film growth process.

2.2. Substrate Preparation and Film Deposition via SILAR

Flexible stainless steel (SS 304) strips, cut to dimensions of 1 cm × 2 cm, were used as substrates for electrode fabrication. To ensure optimal film adhesion and uniformity, a rigorous substrate cleaning protocol was essential. The substrates were sequentially ultrasonicated in analytical-grade acetone, ethanol, and finally deionized water, with each step lasting 10 minutes. This process effectively removed organic residues, particulate matter, and surface oxides. The cleaned substrates were dried under a stream of nitrogen and used immediately for deposition to prevent surface recontamination.

Polyaniline thin films were synthesized using the Successive Ionic Layer Adsorption and Reaction (SILAR) technique, adapted from established methodologies with specific modifications for gas sensing optimization [25]. The SILAR process is a cyclic, layer-by-layer deposition method based on sequential immersion of the substrate into cationic and anionic precursor solutions, with intermediate rinsing steps to remove loosely adsorbed ions. The detailed procedure for a single deposition cycle, illustrated schematically in Figure 1, was as follows:

Adsorption of Aniline: The cleaned stainless steel substrate was immersed in the anionic precursor solution containing 0.5 M aniline and 0.2 M H_2SO_4 for 20 seconds. During this step, aniline monomers and anilinium cations become adsorbed onto the negatively charged substrate surface via electrostatic interaction.

First Rinsing: The substrate was removed from the aniline solution and rinsed thoroughly with doubly distilled water for 10 seconds to eliminate any excess, unadsorbed aniline molecules, ensuring a monolayer formation.

Reaction/Oxidation: The substrate was then transferred to the cationic precursor solution of 0.5 M ammonium persulfate (APS) for 20 seconds. The adsorbed aniline layer reacts with the oxidizing agent (APS). This step initiates the oxidative polymerization, where APS transforms aniline into radical cations that couple to form oligomers and, subsequently, polyaniline chains directly on the substrate surface.

Second Rinsing: Following oxidation, the substrate was again rinsed with doubly distilled water for 10 seconds to stop the reaction by removing excess APS and any by-products, completing one full SILAR cycle.

This four-step sequence constitutes one cycle. To systematically control film thickness and morphology, the process was repeated for 10, 15, and 20 cycles on separate substrates. The H_2SO_4 in the aniline solution concurrently acts as a dopant, protonating the imine nitrogen atoms in the growing polymer chain and stabilizing the conductive emeraldine salt phase. After the final cycle, the coated substrates were washed with distilled water and dried under dynamic vacuum at ambient temperature for 12 hours to yield robust, adherent PANI thin films.

2.3. Characterization Techniques

The structural, morphological, optical, and electrical properties of the SILAR-synthesized PANI films were characterized using a suite of analytical techniques to correlate material properties with sensor performance. The crystalline structure and phase identification were examined using X-ray diffraction (XRD) with a Cu Kα radiation source (λ = 1.5406 Å), scanning over a 2θ range of 10° to 60°. The surface morphology and nanoscale texture of the films were investigated using field emission scanning electron microscopy (FESEM). Optical absorption characteristics were studied via ultraviolet-visible (UV-Vis) spectroscopy in the wavelength range of 200 to 800 nm to identify electronic transitions characteristic of different PANI oxidation states.

The gas sensing properties were evaluated using a custom-built, computer-interfaced static gas sensing system at room temperature (25 ± 2 °C) and relative humidity of 50 ± 5%. The sensing element was prepared by attaching electrical contacts to the PANI-coated substrate using conductive silver paste. The sensor was placed in a sealed glass test chamber of 250 ml volume. Known concentrations of the target volatile organic compounds, acetone, methanol, ammonia, and formaldehyde, were injected into the chamber

 © Ariston Publications 2025. All rights reserved

using a micro-syringe to achieve parts-per-million (ppm) levels, starting from a commercially procured 1000 ppm base concentration in synthetic air. The sensor's electrical resistance was monitored in real-time using a high-precision Keithley 6514 System Electrometer. The sensor response (S) was defined as $S\ (\%) = |(R_g - R_a) / R_a| \times 100$, where R_a is the stable resistance in ambient air and R_g is the resistance upon exposure to the target gas. Key performance metrics, including response magnitude, selectivity, response time (τ_{res}, defined as the time to reach 90% of the maximum response change), and recovery time (τ_{rec}, defined as the time to recover to 90% of the baseline resistance after gas removal), were extracted from the dynamic resistance curves.

3. RESULTS AND DISCUSSION

3.1. Structural and Optical Characterization

The foundational properties of the synthesized polyaniline films, which dictate their electronic and sensing behavior, were elucidated through X-ray diffraction and ultraviolet-visible spectroscopy.

3.1.1. X-ray Diffraction Analysis

The crystallographic structure of the SILAR-deposited PANI thin film was investigated using X-ray diffraction, with the resulting pattern presented in Figure 2 (a). The diffraction profile is dominated by a single, broad halo-like peak centered at a 2θ value of approximately 25.3°. This prominent feature is a well-documented signature of polyaniline, specifically corresponding to diffraction from the (110) crystallographic plane of the polymer's emeraldine salt phase, which aligns with standard reference data (JCPDS card No. 00-060-1167) [26]. The absence of sharp, discrete Bragg peaks and the pronounced broadening of the observed reflection are indicative of a semi-crystalline material. This structure arises from a combination of periodic order along the conjugated polymer backbone and the partial, parallel alignment of adjacent polymer chains, while significant regions remain amorphous due to chain folding and entanglement [27]. The broad nature of the peak directly suggests a nanostructured morphology, where small, ordered crystalline domains are embedded within a dominant amorphous matrix. This semi-crystalline architecture is highly advantageous for gas sensing applications. The amorphous regions provide a porous, accessible network for the rapid diffusion and physical adsorption of gas molecules. Concurrently, the periodic crystalline domains facilitate efficient intra-chain and inter-chain charge transport, which is essential for translating a surface adsorption event into a measurable change in the film's bulk electrical resistance. Therefore, the XRD data confirm the successful synthesis of PANI in its conductive form and highlight a material structure intrinsically suited for room-temperature chemiresistive sensing.

3.1.2. Ultraviolet-Visible Spectroscopy

The electronic structure and optical properties of the PANI film were probed using UV-Vis absorption spectroscopy, as shown in Figure 2(b). The absorption spectrum exhibits two primary characteristic bands. The first is a strong, well-defined peak appearing in the ultraviolet region between 230 and 250 nm.

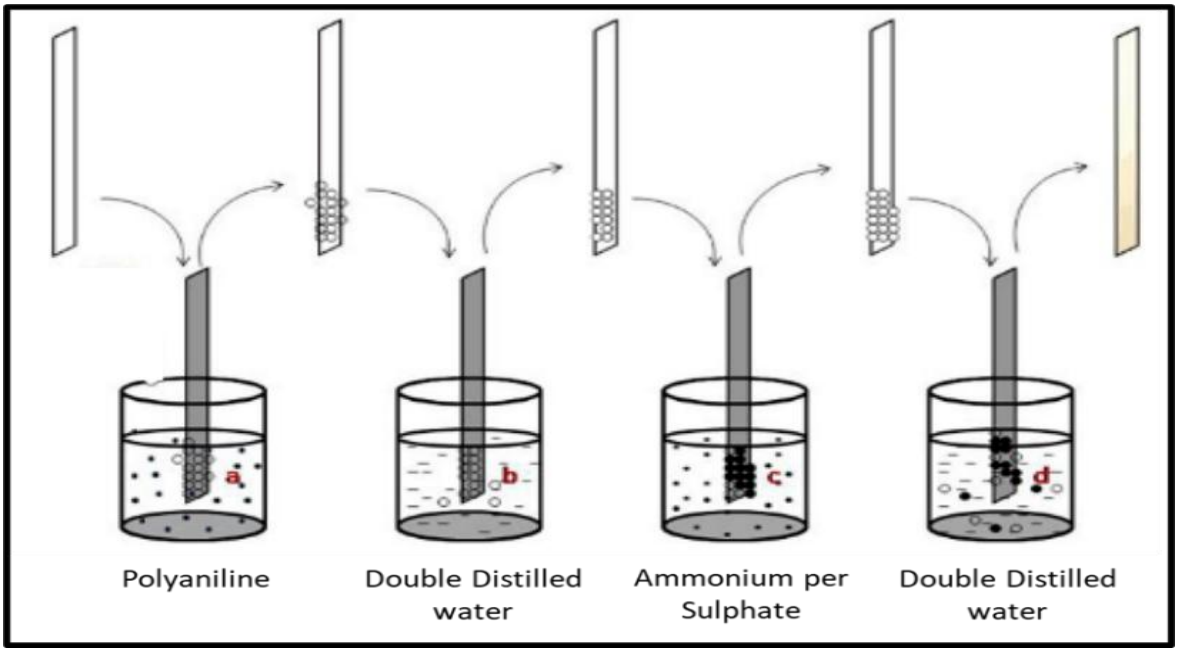

Fig. 1. Schematic of the SILAR method for polyaniline (PANI) thin film deposition.

© Ariston Publications 2025. All rights reserved.

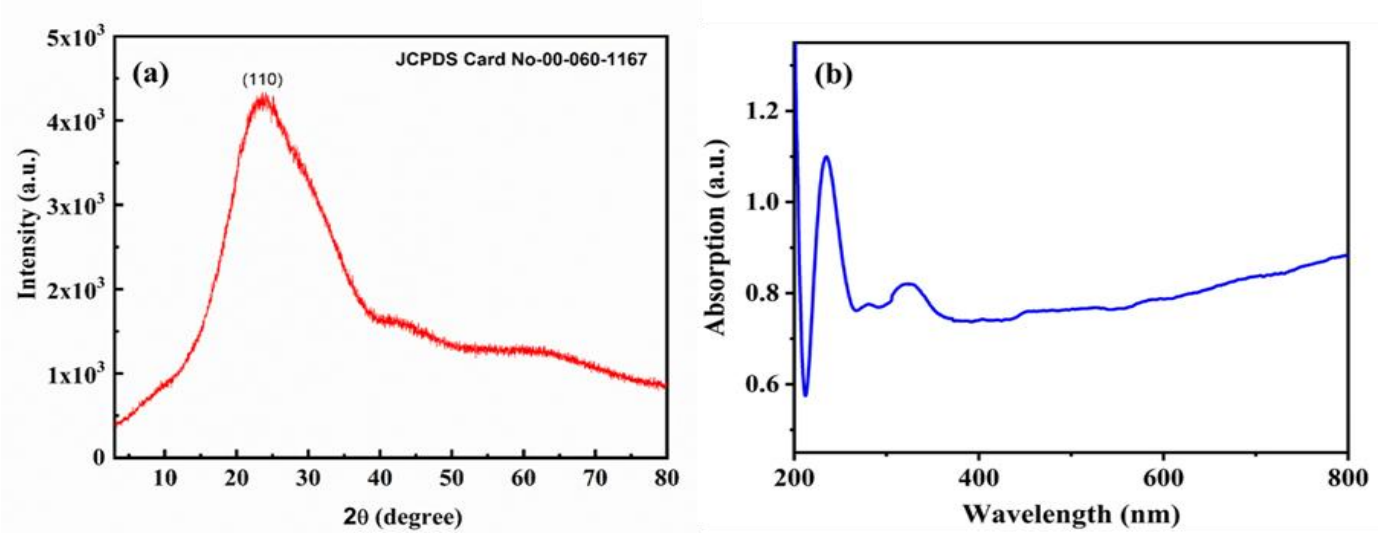

Fig. 2. (a) XRD pattern and (b) UV-Vis spectrum of the synthesized PANI thin film.

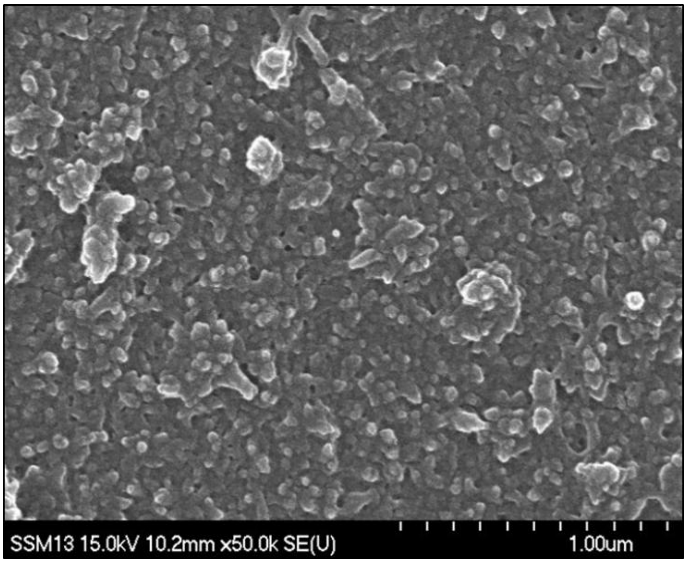

Fig. 3. SEM image showing the porous, granular morphology of the PANI film.

This absorption band is attributed to the π-π* electronic transition within the benzenoid rings of the aniline monomer units, a feature fundamental to the aromatic character of the polymer backbone.

The second distinct feature is a broader absorption band spanning the 320-360 nm range. This band is associated with polaronic transitions, specifically the π-polaron or exciton-type transition, which is a definitive signature of the doped, conductive emeraldine salt form of PANI. The presence of this polaron band confirms successful protonic acid doping by H_2SO_4 during the SILAR synthesis, leading to the generation of charge carriers (polarons/bipolarons) along the polymer chain. Furthermore, the spectrum shows a steady increase in absorption extending into the visible region (400-800 nm). This tailing absorption is indicative of extensive π-conjugation and charge carrier delocalization along the polymer backbone, a direct consequence of the doping process. This extended conjugation is critical for gas sensing, as it establishes a sensitively tunable electronic pathway. The interaction with electron-withdrawing or electron-donating gas molecules can effectively modulate this conjugated system, leading to significant and detectable changes in the film's electrical conductivity.

3.2. Surface Morphology Analysis by Scanning Electron Microscopy

The surface topography and nanoscale morphology of the PANI film, crucial factors governing its gas interaction dynamics, were examined using scanning electron microscopy. The representative SEM micrograph in Figure 3 reveals a uniform and densely packed granular morphology. The film is composed of interconnected, nanosized primary grains that aggregate to form a highly porous, three-dimensional network. These spherical or elliptical grains, with dimensions in the nanometer range, are interspersed with larger, irregularly shaped agglomerates. This agglomeration is a typical phenomenon in polymer thin films and can be ascribed to the layer-by-layer growth mechanism of the SILAR process. During successive cycles, newly formed polymer chains nucleate on existing grains, leading to cluster growth and some degree of localized chain entanglement.

This specific morphology is exceptionally favorable for gas sensing. The nanoscale granularity and the interstitial pores between grains collectively create a high surface-to-volume ratio. This maximized surface area provides an abundant number of active sites for the adsorption of target gas molecules. Moreover, the porous network facilitates the

 © Ariston Publications 2025. All rights reserved

rapid inward diffusion of analyte molecules and the efficient outward diffusion of desorbed species, ensuring the entire film volume participates in the sensing reaction. The micrograph also shows a continuous film coverage without major cracks or pinholes, indicating good structural integrity and adhesion to the stainless-steel substrate. This uniformity is essential for achieving stable and reproducible electrical contacts and consistent sensor performance over multiple measurement cycles.

3.3. Gas Sensing Performance Evaluation

The room-temperature chemiresistive sensing performance of the SILAR-fabricated PANI film was rigorously evaluated, with a principal focus on the detection of acetone vapor.

3.3.1. Selectivity Profile

The fundamental requirement for a practical sensor is its ability to distinguish a target analyte from other interfering gases. The selectivity of the PANI sensor was assessed by exposing it to four different volatile organic compounds, acetone, methanol, ammonia, and formaldehyde, each at an identical concentration of 100 ppm. The corresponding sensor response magnitudes are compared in Figure 4 (a). The sensor demonstrated a distinct and pronounced preference for acetone, yielding a maximum response of 85%. Under the same conditions, the responses to methanol, ammonia, and formaldehyde were significantly lower, recorded at 78%, 55%, and 48%, respectively. This superior selectivity for acetone can be rationalized by considering the interplay of molecular and material properties. Acetone possesses a strong dipole moment and a carbonyl (C=O) group that can engage in specific dipole-dipole interactions and weak hydrogen bonding with the imine and amine nitrogen sites on the PANI backbone. Furthermore, its moderate electron-withdrawing nature leads to an efficient charge transfer interaction with the p-type PANI, resulting in a measurable increase in resistance. While methanol can also interact via hydrogen bonding, its smaller size and different polarity may lead to weaker or less specific adsorption. Ammonia, a strong electron donor, typically causes a sharp decrease in PANI's resistance, but the observed lower response suggests the film's morphology and doping level may be less optimized for this strong base. Formaldehyde's lower response is likely due to its high reactivity and potential for different interaction mechanisms. The porous, high-surface-area morphology achieved via SILAR deposition accentuates these subtle differences in interaction strength, thereby enhancing selectivity.

3.3.2. Concentration-Dependent Sensitivity

The quantitative sensing capability of the PANI film was investigated by measuring its response to varying concentrations of acetone, ranging from 10 ppm to 100 ppm. The results, plotted in Figure 4(b), exhibit a clear and monotonic increase in sensor response with rising acetone concentration. The response initiated at 44% for 10 ppm and progressed steadily to 51% (20 ppm), 65% (50 ppm), and finally saturated near 85% at 100 ppm. This positive correlation follows a trend expected for surface-adsorption-dominated sensing mechanisms. At lower concentrations, the available active sites on the PANI surface are in excess relative to the number of analyte molecules, leading to a sub-linear increase in response. As the concentration rises, more adsorption sites become occupied, causing a more pronounced change in the film's electronic structure and, consequently, its resistance. The absence of saturation within this tested range (10-100 ppm) indicates the sensor's utility for quantitative analysis across concentrations relevant for both environmental monitoring, such as industrial leaks, and medical diagnostics for instance, breath acetone in diabetes, typically 1-10 ppm but higher in ketoacidosis. The consistent trend also underscores the reproducibility and reliability of the film's fabrication process.

3.3.3. Dynamic Response and Recovery Kinetics

The practical utility of a sensor is also determined by its speed and reversibility. The dynamic transient response curve for the PANI sensor upon exposure to 100 ppm acetone is presented in Figure 4 (c). Upon acetone injection, the sensor resistance increased sharply, reaching 90% of its maximum change in approximately 219.6 seconds. This response time (τ_{res}) reflects the combined kinetics of gas diffusion through the porous film, adsorption onto active sites, and the subsequent charge transfer process. The value of ~220 seconds indicates a reasonably rapid adsorption process, facilitated by the film's open nanostructure. Upon the removal of acetone and the reintroduction of clean air, the resistance gradually returned to its original baseline. The time required to recover 90% of the initial baseline resistance was approximately 444.4 seconds. The recovery time (τ_{rec}) is typically longer than the response time, as it involves the desorption of chemically or physically bound acetone molecules, which is a process often requiring more activation energy. The fact that recovery is achieved completely, as evidenced by the return to the original baseline, confirms the interaction is predominantly reversible and physical (physisorption) in nature, rather than irreversible chemical binding. This reversibility is crucial for the reusable operation of the sensor. The ratio of recovery to response time suggests that while adsorption is efficient, future work could focus on modifying the polymer's surface chemistry or employing mild heating to accelerate desorption for faster cycle times [28]. Nevertheless, the demonstrated combination of high selectivity (85%), good sensitivity across a relevant concentration range, and reversible operation at room temperature validates the SILAR-synthesized PANI thin film as a highly promising platform for developing energy-efficient acetone sensors.

© Ariston Publications 2025. All rights reserved.

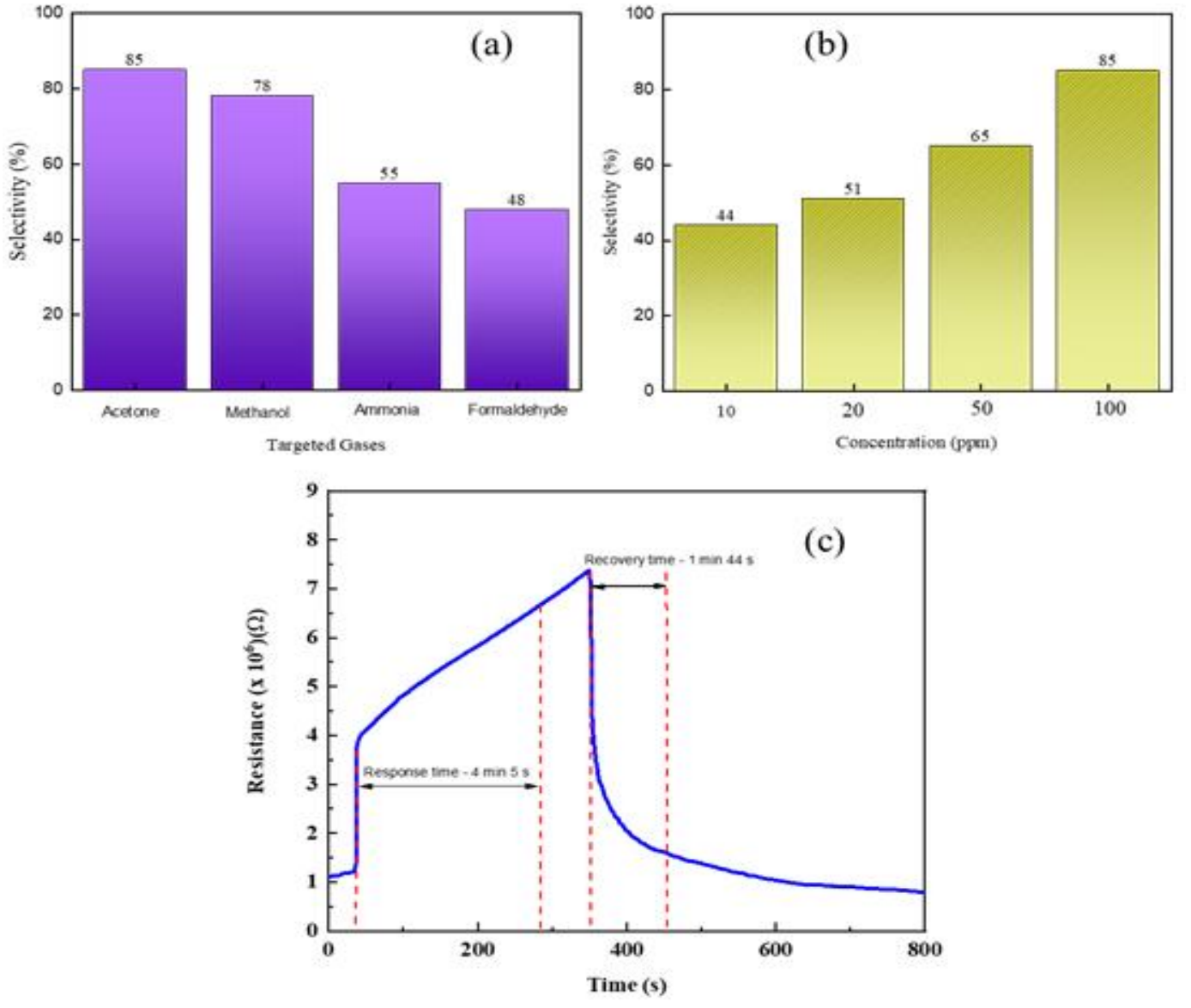

Fig. 4. Acetone sensing performance: (a) selectivity to various VOCs, (b) concentration-dependent response, and (c) dynamic response-recovery transient.

4. CONCLUSION

This investigation successfully established the efficacy of polyaniline thin films, synthesized via the SILAR method, as functional acetone gas sensors operating at ambient temperature. Detailed structural and morphological characterizations through XRD and SEM confirmed the formation of a semicrystalline PANI matrix with a porous, granular morphology. This unique nanostructure provides a high surface area conducive to the adsorption and diffusion of gas molecules, which is fundamental to the sensing mechanism. The fabricated sensor displayed exceptional selectivity for acetone, registering an 85% response, which surpassed its sensitivity toward methanol, ammonia, and formaldehyde. The sensor response exhibited a direct correlation with acetone concentration, achieving its maximum sensitivity of 85% at 100 ppm. Kinetic evaluation revealed a response time of roughly 219.6 seconds and a recovery period of approximately 444.4 seconds for 100 ppm acetone, demonstrating reasonably rapid and reversible interaction between the acetone vapor and the PANI active sites. Collectively, these attributes highlight the suitability of SILAR-derived PANI films for selective, low-power, and room-temperature acetone detection. The implications of this work are particularly relevant for non-invasive diagnostic platforms, such as breath analyzers for diabetes monitoring, as well as for real-time environmental surveillance of volatile organic compounds. Future efforts will focus on enhancing the long-term stability and reproducibility of the sensors, exploring their responsiveness to a broader spectrum of gases, and integrating them into multiplexed or flexible sensing arrays for practical field applications.

 © Ariston Publications 2025. All rights reserved

DECLARATIONS

Ethical Approval

We affirm that this manuscript is an original work, has not been previously published, and is not currently under consideration for publication in any other journal or conference proceedings. All authors have reviewed and approved the manuscript, and the order of authorship has been mutually agreed upon.

Funding
Not applicable

Availability of data and material

The datasets generated and/or analyzed during the current study are available from the corresponding author upon reasonable request.

Conflicts of Interest

The authors declare that they have no financial or personal interests that could have influenced the research and findings presented in this paper. The authors alone are responsible for the content and writing of this article.

Authors' contributions

All authors contributed equally to this work.

REFERENCES

[1] Kotnana, G. and Hong, S., **2025.** Recent progress on rare earth orthoferrites for gas-sensing applications. *Chemosensors*, 13(5), pp.156. doi:10.3390/chemosensors13050156.

[2] Sundriyal, S., Shrivastav, V., Kaur, H., Mishra, S. and Deep, A., **2018.** High-performance symmetrical supercapacitor with a combination of a ZIF-67/rGO composite electrode and a redox additive electrolyte. *ACS Omega*, 3(12), pp.17348–17358. doi:10.1021/acsomega.8b02065.

[3] Gaikar, P.S., et al., **2017.** A simple wet-chemical synthesis, reaction mechanism, and charge storage application of cobalt oxide electrodes of different morphologies. *Electrochimica Acta*, 253, pp.151–162. doi:10.1016/j.electacta.2017.09.039.

[4] MacDonald, M., Thoma, E., George, I. and Duvall, R., **2022.** Demonstration of VOC fenceline sensors and canister grab sampling near chemical facilities in Louisville, Kentucky. *Sensors*, 22(9), pp.3480. doi:10.3390/s22093480.

[5] Ho, C.K., Robinson, A., Miller, D.R. and Davis, M.J., **2005.** Overview of sensors and needs for environmental monitoring. *Sensors*, 5(1), pp.4–37. doi:10.3390/s5010004.

[6] Navale, S.T., et al., **2017.** Solution-processed rapid synthesis strategy of Co_3O_4 for the sensitive and selective detection of H_2S. *Sensors and Actuators B: Chemical*, 245, pp.524–532. doi:10.1016/j.snb.2017.01.195.

[7] Arulvasan, W., et al., **2024.** High-quality identification of volatile organic compounds (VOCs) originating from breath. *Metabolomics*, 20(5), pp.102. doi:10.1007/s11306-024-02163-6.

[8] Li, C., Choi, P.G., Kim, K. and Masuda, Y., **2022.** High performance acetone gas sensor based on ultrathin porous NiO nanosheet. *Sensors and Actuators B: Chemical*, 367, pp.132143. doi:10.1016/j.snb.2022.132143.

[9] Chen, Y. and Cao, Y., **2020.** Ultrasensitive and low detection limit of acetone gas sensor based on ZnO/SnO_2 thick films. *RSC Advances*, 10(59), pp.35958–35965. doi:10.1039/D0RA06406H.

[10] Amiri, V., Roshan, H., Mirzaei, A., Neri, G. and Ayesh, A.I., **2020.** Nanostructured metal oxide-based acetone gas sensors: A review. *Sensors*, 20(11), pp.3096. doi:10.3390/s20113096.

[11] Zhang, H., Liu, L., Huang, C., Liang, S. and Jiang, G., 2023. Enhanced acetone gas sensing performance of ZnO polyhedrons decorated with $LaFeO_3$ nanoparticles. *Materials Research Express*, 10(9), pp.095902. doi:10.1088/2053-1591/acf6f8.

[12] Majhi, S.M., Mirzaei, A., Kim, H.W., Kim, S.S. and Kim, T.W., **2021.** Recent advances in energy-saving chemiresistive gas sensors: A review. *Nano Energy*, 79, p.105369. doi:10.1016/j.nanoen.2020.105369.

[13] Anisimov, Y.A., Evitts, R.W., Cree, D.E. and Wilson, L.D., **2021.** Polyaniline/biopolymer composite systems for humidity sensor applications: A review. *Polymers*, 13(16), pp.2722. doi:10.3390/polym13162722.

[14] Tan, W., Stallard, J.C., Jo, C., De Volder, M.F.L. and Fleck, N.A., **2021.** The mechanical and electrochemical properties of polyaniline-coated carbon nanotube mat. *Journal of Energy Storage*, 41, p.102757. doi:10.1016/j.est.2021.102757.

© Ariston Publications 2025. All rights reserved.

[15] Kulkarni, V.G., **1999.** Polyanilines: Progress in processing and applications. In: *Polyanilines: Progress in Processing and Applications*. ACS Publications, pp.174–183. doi:10.1021/bk-1999-0735.ch012.

[16] Agbor, N.E., Petty, M.C. and Monkman, A.P., **1995.** Polyaniline thin films for gas sensing. *Sensors and Actuators B: Chemical*, 28(3), pp.173–179. doi:10.1016/0925-4005(95)01725-9.

[17] Li, G. and Semancik, S., **2005.** Electrophoretic integration of polyaniline on NIST microhotplate for gas sensing. *MRS Proceedings*, 876, pp.R6.9. doi:10.1557/PROC-876-R6.9.

[18] Suryawanshi, V.B., Bobade, R.G., Gaikwad, D.S., Nakate, U.T., Shaikh, S.F., Lokhande, B.J. and Ambare, R.C., **2024.** Nano-architectured BaO thin film electrode synthesized via SILAR technique for supercapacitor application. *Chemical Papers*, 78(8), pp.4689–4697. doi:10.1007/s11696-024-03556-6.

[19] Fan, L., Zhu, B., Su, P.C. and He, C., **2018.** Nanomaterials and technologies for low temperature solid oxide fuel cells: Recent advances, challenges and opportunities. *Nano Energy*, 45, pp.148–176. doi:10.1016/j.nanoen.2017.12.044.

[20] Li, Y., Jiao, M., Zhao, H. and Yang, M., **2018.** High performance gas sensors based on in-situ fabricated ZnO/polyaniline nanocomposite: The effect of morphology on the sensing properties. *Sensors and Actuators B: Chemical*, 264, pp.285–295. doi:10.1016/j.snb.2018.02.157.

[21] Lin, Q., Li, Y. and Yang, M., **2012.** Gas sensing properties of layer-by-layer self-assembled ultrathin film of polyaniline/titanium dioxide. *Synthetic Metals*, 162(24), pp.2242–2249. doi:10.1016/j.synthmet.2012.09.026.

[22] Feng, Q., Zhang, H., Shi, Y., Yu, X. and Lan, G., **2021.** Preparation and gas sensing properties of PANI/SnO_2 hybrid material. *Polymers*, 13(9), p.1360. doi:10.3390/polym13091360.

[23] Abdollahi-Alibeik, M., Moosavifard, M. and Poorirani, S., **2013.** Synthesis of 2-substituted benzimidazoles in the presence of polyaniline nanoparticles doped with 12-tungstophosphoric acid as reusable heterogeneous catalyst. *Synthesis and Reactivity in Inorganic, Metal-Organic, and Nano-Metal Chemistry*, 43(10), pp.1365–1371. doi:10.1080/15533174.2012.761233.

[24] Khudiar, S.S., Nayef, U.M., Mutlak, F.A.H. and Abdulridha, S.K., **2022.** Characterization of NO_2 gas sensing for ZnO nanostructure grown hydrothermally on porous silicon. *Optik*, 249, pp.168300. doi:10.1016/j.ijleo.2021.168300.

[25] Angre, A.P., Gaikar, P., Patil, P.G., Kim, H.W., Kim, J.M. and Bulakhe, R.N., **2025.** SILAR synthesized polyaniline flexible thin-film electrodes with different oxidizing agents for supercapacitor applications. *Journal of Materials Science: Materials in Electronics*, 36(23), pp.1437. doi:10.1007/s10854-025-15518-z.

[26] Saouti, F., Belaaouad, S., Cherqaoui, A. and Naimi, Y., **2021.** Polyaniline thin film prepared by electrochemical polymerization method. *Biointerface Research in Applied Chemistry*, 12(4), pp.5523–5533. doi:10.33263/BRIAC124.55235533.

[27] Luzny, W., Banka, E. and Stochmal-Pomarzanska, E., **2000.** Structure of polyanilines: the review of some recent results. In: Wlochowicz, A. (Ed.), *Proceedings of SPIE*, pp.47–50. doi:10.1117/12.401850.

[28] Li, L., Diao, Q., Liu, Z., Zhu, G., Jiao, M., Liu, C., Du, M., Shi, Y., Wang, Y., Cheng, P. and Xu, X., **2025.** Preparation of Co_3O_4 by tunable oxygen defect engineering and its application in acetone gas sensor. *Microchemical Journal*, *212*, p.113481. doi:10.1016/j.microc.2025.113481.

 © Ariston Publications 2025. All rights reserved